Fe^+-Mediated Interconversion of *n*- and *i*-C_3H_7OH Preceding Their Gas-Phase Dehydrations: Experimental and Computational Evidence for Memory Effects and Inherent Asymmetry of Constitutionally Equivalent Methyl Groups†,‡

Claudia Trage, Detlef Schröder, and Helmut Schwarz*

Institut für Chemie, Technische Universität Berlin, Strasse des 17. Juni 135, D-10623 Berlin, Germany

Received October 28, 2002

The *n*-propyl/isopropyl isomerization operative in Fe^+-mediated dehydrations of *n*-propyl and isopropyl alcohols has been rigorously analyzed by tandem mass spectrometry and density functional calculations. Metastable ion studies of complexes of atomic Fe^+ with a set of selectively deuterated propyl alcohols address structural details of the reversibility of β-hydrogen transfer steps. The labeling distributions in the ionic products reveal that the transiently focused, constitutionally equivalent methyl groups remain distinguishable in the course of *n*-C_3H_7 → *i*-C_3H_7 isomerizations. This asymmetry causes a memory effect operative in the Fe^+-mediated dehydration of *n*-propyl alcohol. While density functional calculations provide detailed insight into the nature of the reaction intermediates and, inter alia, suggest that the experimentally deduced asymmetry can be attributed to agostic interactions of the iron center with a β-hydrogen atom of the emerging methyl group, a comprehensively consistent, quantitative explanation of the experimentally observed effects cannot be provided by the calculations.

1. Introduction

Isotopic labeling experiments represent a time-honored, valuable tool in the elucidation of reaction mechanisms.[1] In organometallic reactions, however, the interpretation of labeling studies is often hampered by extensive H/D equilibrations. In this respect, C−H bond activations at various positions relative to the metal can occur, where the β-hydrogen transfer reaction (Scheme 1) is of particular importance. In many cases, the transition structure of this ubiquitous process already becomes apparent in the related minima, in that these bear unusually small distances between the metal and one of the β-hydrogen atoms: i.e., a β-agostic interaction is operative.[2] The β-agostic binding as well as β-hydrogen transfer benefits from a proper alignment of the C−C backbone of the alkyl substituent; optimal orbital overlap can occur in the case of a planar arrangement of the metal, the migrating hydrogen, and the two carbon atoms connecting them.[3,4]

Particularly promising for uncovering mechanistic features of ionic reactions is the combination of mass spectrometric experiments with computational studies, thereby revealing the intrinsic physical and chemical properties of the system of interest under idealized conditions: i.e., strictly defined ligand-, solvent-, counterion-, and bulk-free species. As far as experimental investigations of the gas-phase chemistry of transition-metal ions are concerned, the pioneering labeling studies of Allison and Ridge[5,6] have already revealed the occurrence of extensive H/D equilibrations in formal 1,2-eliminations of HX (X = halogen, OH, NH_2) upon interaction of various transition-metal cations with alkyl halides, alcohols, and amines. In most of these cases, the observed isotope distributions neither indicate a particularly specific reaction nor agree with complete H/D equilibration: see, for example, the reactions of alcohols and amines with Fe^+, Co^+, and Ni^+.[7] In such situations, the occurrence of H/D exchange processes is often described phenomenologically, while any quantitative analysis is avoided.

Scheme 1

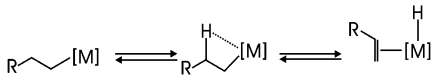

The present work reports a more detailed investigation of the reactions of atomic Fe^+ with *n*-propyl and

* To whom correspondence should be addressed. E-mail: Helmut.Schwarz@www.chem.TU-Berlin.de. Fax: +493031421102.

† Dedicated to Gerhard Quinkert on the occasion of his 75th birthday.

‡ For a short communication, see: Trage, C.; Zummack, W.; Schröder, D.; Schwarz, H. *Angew. Chem., Int. Ed.* **2001**, *40*, 2708.

(1) Kuck, D. *Int. J. Mass Spectrom.* **2002**, *213*, 101.
(2) (a) Cotton, F. A.; LaCour, T.; Stanislowski, A. G. *J. Am. Chem. Soc.* **1974**, *96*, 754. (b) Brookhart, M.; Green, M. L. H. *J. Organomet. Chem.* **1983**, *250*, 395. (c) Cotton, F. A. *Inorg. Chem.* **2002**, *41*, 653.
(3) Versluis, L.; Ziegler, T.; Fan, I. *Inorg. Chem.* **1990**, *29*, 4530.
(4) Veillard, A. *Chem. Rev.* **1991**, *91*, 743.
(5) Allison, J.; Ridge, D. P. *J. Am. Chem. Soc.* **1976**, *98*, 7445.
(6) Allison, J.; Ridge, D. P. *J. Am. Chem. Soc.* **1979**, *101*, 4998.
(7) (a) Prüsse, T.; Schwarz, H. *Organometallics* **1989**, *8*, 2856. (b) Karrass, S.; Prüsse, T.; Eller, K.; Schwarz, H. *J. Am. Chem. Soc.* **1989**, *111*, 9018 and references therein.

10.1021/om020893z CCC: $25.00
Publication on Web 01/21/2003

Chart 1

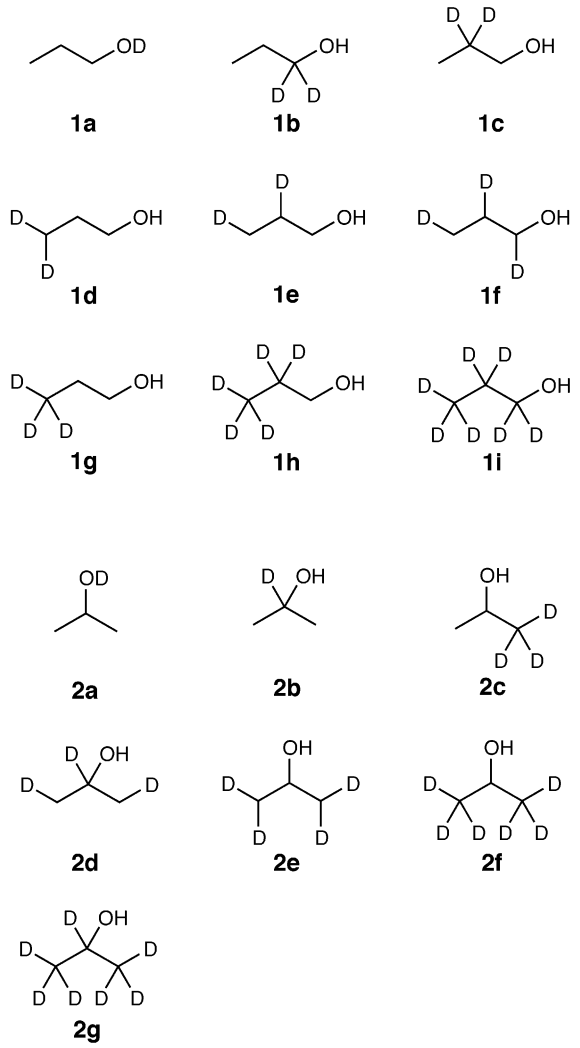

isopropyl alcohol. A suitably large set of deuterated precursors (Chart 1) permits a rigorous quantitative analysis of the labeling experiments. These substrates were chosen on the following grounds (i) The *n*-propyl and isopropyl systems have the minimum size for the exploration of the mechanistic features of transition-metal-mediated backbone equilibration of alkyl chains en route to dehydration. (ii) At the same time, the size of the system is small enough to permit a reasonably straightforward quantum-chemical treatment using density functional theory (DFT).[8] (iii) Finally, the analysis of the *n*-propyl alcohol/Fe^+ and isopropyl alcohol/Fe^+ systems may provide deeper insight into mechanistic aspects of the C−H bond activation of propane by the FeO^+ cation,[9] because oxygenation of propane by FeO^+ proceeds conceptually via the same intermediates accessed from the propyl alcohol/Fe^+ isomers en route to loss of water. In addition, hydroxylation of propane is of particular mechanistic interest, because it is the smallest alkane substrate for which C−H bond activation by a transition-metal oxo species can occur at two chemically distinct positions: i.e., primary and secondary C−H bonds.[10]

(8) Koch, W.; Holthausen, M. C. *A Chemist's Guide to Density Functional Theory*; Wiley-VCH: Weinheim, Germany, 2000.
(9) Jackson, T. C.; Jacobson, D. B.; Freiser, B. S. *J. Am. Chem. Soc.* **1984**, *106*, 1252.

2. Experimental Details

2.1. Mass Spectrometric Investigations. Most experiments were performed with a modified four-sector tandem mass spectrometer of BEBE configuration (B and E stand for magnetic and electric sectors, respectively), in which MS-I is a VG ZAB-HF-2F spectrometer and MS-II an AMD 604 mass spectrometer.[11−13] In brief, ions of interest were generated by chemical ionization (CI) of ca. 1:1 mixtures of $Fe(CO)_5$ and the desired propyl alcohols, bombarded with electrons having 100 eV electron energy. The resulting Fe^+/C_3H_7OH complexes, whose precise genesis is unknown, were accelerated to 8 keV kinetic energy and mass selected by using B(1) and E(1). Unimolecular dissociations of metastable ions (MI) occurring in the field-free region between E(1) and B(2) were recorded by scanning B(2). Collisional activation (CA) mass spectra were obtained similarly with helium as a target gas (80% transmission).

Additional gas-phase studies were performed with a Spectrospin CMS 47X Fourier transform ion cyclotron resonance (FTICR) mass spectrometer described elsewhere.[14,15] In brief, Fe^+ cations were formed by laser desorption/laser ionization of iron in an external ion source and transferred to the analyzer cell located in a superconducting magnet with a maximum field strength of 7.05 T. Subsequently, $^{56}Fe^+$ was mass selected using the FERETS technique,[16] a computer-controlled ion-ejection protocol which combines single-frequency ion-ejection pulses with frequency sweeps to optimize ion isolation. Next, Fe^+ was converted to FeO^+ by pulsing in N_2O,[17] which also serves as a cooling gas.[18] After removal of N_2O, the FeO^+ cation was mass selected and trapped in propane which was introduced into the FTICR cell by a leak valve at typical pressures of $(4-10) \times 10^{-9}$ mbar. Reaction rate constants and branching ratios were derived from an analysis of the pseudo-first-order reaction kinetics. For the conversion of the experimentally measured rate constants to the absolute values, the measured pressures were corrected according to the relative sensitivity of the ion gauge, which was calibrated using data reported for well-known ion/molecule processes.[18] Note, however, that several systematic errors cancel in the relative rate constant measurements discussed below and an error estimate of ±10 is indicated.[19] For the evaluation of precise intensities in the case of isobaric multiplets, exact ion masses were determined by high-resolution experiments ($m/\Delta m$ > 200 000), and intensities were derived from the absolute amplitudes of the transients. Furthermore, all ion intensities were deconvoluted to take into account natural abundances of all relevant isotopes and to correct for the incompleteness of deuterium labeling.

2.2. Synthetic Procedures. The synthesis of the labeled propyl alcohols **1a**−**i** and **2a**−**g** (Chart 1) followed well-established preparative procedures and is therefore not discussed in detail. In brief, the [O−D]-propyl alcohols **1a** and **2a** were prepared by treatment of the corresponding sodium

(10) Schröder, D.; Schwarz, H. *Angew. Chem., Int. Ed. Engl.* **1995**, *34*, 1973.
(11) Schalley, C. A.; Schröder, D.; Schwarz, H. *Int. J. Mass Spectrom. Ion Processes* **1996**, *153*, 173.
(12) Srinivas, R.; Sülzle, D.; Koch, W.; DePuy, C. H.; Schwarz, H. *J. Am. Chem. Soc.* **1991**, *113*, 5970.
(13) Srinivas, R.; Sülzle, D.; Weiske, T.; Schwarz, H. *Int. J. Mass Spectrom. Ion Processes* **1991**, *107*, 368.
(14) Eller, K.; Schwarz, H. *Int. J. Mass Spectrom. Ion Processes* **1989**, *93*, 243.
(15) Eller, K.; Zummack, W.; Schwarz, H. *J. Am. Chem. Soc.* **1990**, *112*, 621.
(16) Forbes, R. A.; Laukien, F. H.; Wronka, J. *Int. J. Mass Spectrom. Ion Processes* **1988**, *83*, 23.
(17) Kappes, M.; Staley, R. H. *J. Am. Chem. Soc.* **1981**, *103*, 1286.
(18) Schröder, D.; Schwarz, H.; Clemmer, D. E.; Chen, Y.; Armentrout, P. B.; Baranov, V. I.; Böhme, D. K. *Int. J. Mass Spectrom. Ion Processes* **1997**, *161*, 177.
(19) Schröder, D. Ph.D. Thesis, Technische Universität Berlin, D83, 1992.

propanolates with D_2O. **1b**,**c**,**h**,**i** were made by reduction of the corresponding acids with $LiAlH_4$ and $LiAlD_4$, respectively. Catalytic reduction of unlabeled and [1-D_1]-prop-2-en-1-ol with deuterium afforded **1e**,**f**, respectively; the required labeled allyl alcohol was obtained by reduction of acrolein with $LiAlD_4$. **1d**,**g** were prepared by Cu^I-catalyzed ($CuBr \cdot Me_2S$) addition of the corresponding Grignard reagents to ethylene oxide. Except for the preparation of **2c** by addition of CD_3MgI to acetaldehyde, all labeled isopropyl alcohols were made by reduction of acetone, [D_6]-acetone, 1,3-dichloroacetone, and [1,1,3,3-D_4]-1,3-dichloroacetone with $LiAlH_4$ and $LiAlD_4$, respectively. Note that the synthesis of **1e**,**f** and **2c** yields racemic products. Since traces of most solvents and side products would disturb the mass spectrometric examination of the compounds under study, most of the compounds were purified by preparative gas chromatography.

3. Theoretical Section

3.1. Computational Details. The relevant potential-energy surfaces (PESs) were computed using two different DFT/HF hybrid functionals, namely, the common B3LYP[20,21] approach and the *m*PW1PW91[22] method, both implemented in Gaussian 98.[23] Optimizations of minima and transition structures were carried out at the B3LYP level with double-ζ basis sets for hydrogen, including diffuse and polarization functions for carbon and oxygen (6-31+G*). For iron, the all-electron TZV basis set developed by Ahlrichs and co-workers[24] was used. To identify stationary points as local minima, transition structures, or higher order saddle points, frequency calculations were performed at the same level of theory. Relative energies and population analyses were calculated as single points on the optimized geometries, employing both B3LYP and *m*PW1PW91 functionals with larger triple-ζ basis sets 6-311++G** for the nonmetals. In these calculations, the basis set of iron was augmented by two uncontracted p functions (exponents $\alpha = 0.134\,915$ and $0.041\,843$) and one f function with an exponent of 2.5.[24] For the sake of simplicity, the methods using the smaller basis sets are denoted as DZP and those employing the larger ones will be referred to as TZP. The energies were corrected for zero-point vibrational energies using the unscaled frequencies obtained at the DZP level.

The two different DFT/HF approaches were applied for the following reasons. The B3LYP functional has been shown to provide reasonably accurate geometries and relative energies for many organic as well as several organometallic systems while having modest computational demands.[25,26] The *m*PW1PW91 functional is specifically parametrized to adequately describe weak as well as noncovalent interactions[22] associated with transition structures, while retaining accuracy for the description of covalent bonds. As far as transition metals are concerned, a recent study of Porembski and Weisshaar[27] suggests that the latter method is in fact more suitable to describe coordinatively unsaturated transition-metal compounds. Specifically, the proper description of low-spin/high-spin splitting in 3d atoms is known to pose problems with the B3LYP approach, where iron constitutes a notoriously problematic case. For example, the previously used B3LYP/6-311+G* level of theory[28−30] predicts $Fe^+(^4F, 3d^7)$ to be 17 kJ/mol more stable than $Fe^+(^6D, 4s^13d^6)$, whereas atomic Fe^+ actually has a ^6D ground state according to spectroscopy[31] with the ^4F first excited state 24 kJ/mol higher in energy. Some improvement is achieved with the larger basis set employed in this work, in that B3LYP/TZP gives the correct order of ground and excited states, while the computed state splitting of only 0.1 kJ/mol in favor of $Fe^+(^6D)$ is still much too low. Instead, much better agreement is achieved at the *m*PW1PW91/TZP level of theory, which predicts the Fe^+ (^4F) excited state to be 17 kJ/mol higher in energy than the Fe^+ ^6D ground state.

3.2. Kinetic Modeling Approach. In the present work, the H/D exchange processes observed in the MI mass spectra of propyl alcohol/Fe^+ complexes are not only discussed phenomenologically but also analyzed quantitatively. This is achieved by kinetic modeling using the following systematic approach. The assumed elementary steps in the dehydration of propyl alcohol/Fe^+ are used for constructing several mathematical models which are then probed with respect to their ability to describe the experimental data, specifically the extent of H/D equilibration and associated kinetic isotope effects (KIEs). The mathematical routines inter alia involve a numerical fit of the modeled data to the experimentally observed ratios of the intensities of H_2O and HDO losses by adjusting the parameters involved. The parameters were specified by solving the sets of nonlinear equations with the program Mathcad Professional[32] using a modified Levenberg−Marquard method.[33] A sensitivity analysis is included for the parameters originating from the models which show the best agreement with the experimental data. The quoted errors of the parameters represent the maximum tolerated deviation from the fitted parameter, for which the modeled H_2O/HDO ratios still lay within the experimental error. To determine this maximum tolerated deviation, one of the parameters was varied at a time until the modeled H_2O/HDO ratios exceed the error bars of the experimentally measured H_2O and HDO intensities.

In the following paragraph, the parameters used in the kinetic modeling are defined. Details about the general structure of the kinetic models are given in section 4.2, in which the different models are developed by reference to the experimental results.[34] Briefly, f_s stands for the fraction of the reaction that follows a selective 1,2-elimination. Likewise, $1 - f_s$ stands for the fraction of the reaction where elimination of water takes place after a complete H/D equilibration of the alkyl hydrogen atoms. Furthermore, the measured H_2O/HDO ratios are associated with kinetic isotope effects separated into

(20) Becke, A. D. *J. Chem. Phys.* **1993**, *98*, 5648.
(21) Stephens, P. J.; Devlin, F. J.; Frisch, M. J.; Chabalowski, C. F. *J. Phys. Chem.* **1994**, *98*, 11623.
(22) Adamo, C.; Barone, V. *J. Chem. Phys.* **1998**, *108*, 664.
(23) Frisch, M. J.; Trucks, G. W.; Schlegel, H. B.; Scuseria, G. E.; Robb, M. A.; Cheeseman, J. R.; Zakrzewski, V. G.; Montgomery, J. A., Jr.; Stratmann, R. E.; Burant, J. C.; Dapprich, S.; Millam, J. M.; Daniels, A. D.; Kudin, K. N.; Strain, M. C.; Farkas, O.; Tomasi, J.; Barone, V.; Cossi, M.; Cammi, R.; Mennucci, B.; Pomelli, C.; Adamo, C.; Clifford, S.; Ochterski, J.; Petersson, G. A.; Ayala, P. Y.; Cui, Q.; Morokuma, K.; Malick, D. K.; Rabuck, A. D.; Raghavachari, K.; Foresman, J. B.; Cioslowski, J.; Ortiz, J. V.; Stefanov, B. B.; Liu, G.; Liashenko, A.; Piskorz, P.; Komaromi, I.; Gomperts, R.; Martin, R. L.; Fox, D. J.; Keith, T.; Al-Laham, M. A.; Peng, C. Y.; Nanayakkara, A.; Gonzalez, C.; Challacombe, M.; Gill, P. M. W.; Johnson, B. G.; Chen, W.; Wong, M. W.; Andres, J. L.; Head-Gordon, M.; Replogle, E. S.; Pople, J. A. *Gaussian 98*, revision A.7; Gaussian, Inc.: Pittsburgh, PA, 1998.
(24) Schäfer, A.; Huber, C.; Ahlrichs, R. *J. Chem. Phys.* **1994**, *100*, 5829. URL: ftp://ftp.chemie.uni-karlsruhe.de/pub/basen/fe.
(25) Cundari, T. R., Ed. *Computational Organometallic Chemistry*; Marcel Dekker: New York, 2001.
(26) Henry, D. J.; Radom, L. *Quantum-Mechanical Prediction of Thermochemical Data*; Kluwer: Dordrecht, The Netherlands, 2001; p 161.
(27) Porembski, M.; Weisshaar, J. C. *J. Phys. Chem. A* **2001**, *105*, 4851.
(28) Note that 6-311G specifies the Wachters−Hay all-electron basis set for elements of the first transition row, using the scaling factors of Raghavachari and Trucks: (a) Wachters, A. J. H. *J. Chem. Phys.* **1970**, *52*, 1033. (b) Hay, P. J. *J. Chem. Phys.* **1977**, *66*, 4377. (c) Raghavachari, K.; Trucks, G. W. *J. Chem. Phys.* **1989**, *91*, 1062.
(29) Bärsch, S.; Schröder, D.; Schwarz, H.; Armentrout, P. B. *J. Phys. Chem. A* **2001**, *105*, 2005.
(30) Bärsch, S.; Schröder, D.; Schwarz, H. *Chem. Eur. J.* **2000**, *6*, 1789.
(31) Sugar, J.; Corliss, C. *J. Phys. Chem. Ref. Data* **1985**, *14*, Supplement No. 2. URL: http://physics.nist.gov/PhysRefData/.
(32) Mathcad 8 Professional; MathSoft, Inc., 1986−1998.
(33) More, J. J.; Garbow, B. S.; Hilstrom, K. E. *User's Guide to Minpack I*; Argonne National Laboratory: Argonne, IL, 1980.
(34) Further details are available upon request from: claudia.trage@www.chem.tu-berlin.de.

Chart 2

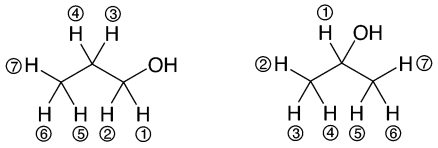

KIE_s and KIE_x to account for the possibility that the two reaction pathways could be associated with different kinetic isotope effects. Here, KIE_s stands for the isotope effect associated with the selective 1,2-elimination pathway and KIE_x for that of dehydration after complete H/D scrambling. Note that possible secondary isotope effects are not considered explicitly, because they are either inherently included in the KIE terms and/or cancel out in the H_2O/HDO ratios for the set of deuterated propyl alcohol/Fe^+ systems examined here, because only a single H/D atom is transferred from the propyl unit (see below). To differentiate between H or D atoms at a certain position, the hydrogen atoms are numbered serially in the manner shown in Chart 2. In the associated algorithms, x_i is assigned the value 1 for deuterium in a position i ($i = 1-7$) and $x_i = 0$ in case of hydrogens. This procedure provides a tool to describe the initial isotopic labeling pattern and therefore enables an assessment of the probability of finding H or D atoms at certain positions of the molecule (C(1), C(2), or C(3)) and of considering statistical weights.

4. Results and Discussion

The paper is organized such that the experimental findings are presented first. Subsequently, the kinetic modeling of the data is discussed, which provides insight into the occurrence and reversibilities of the various elementary steps. Next, the relevant parts of the potential-energy surfaces are explored by quantum-chemical calculations using density-functional theory. Finally, the combined experimental and computational results are used to analyze the experimental data obtained for the related ion/molecule reaction of FeO^+ with propane, where the regioselectivity of the initial C−H bond activation is of particular interest.[10]

4.1. Dissociation of Propyl Alcohol/Fe^+ Complexes. Two pieces of basic information can be gained immediately from the examination of the dissociation reactions of the mass-selected complexes of Fe^+ with unlabeled *n*-propyl and isopropyl alcohol, respectively. First, loss of water is by far the most dominant reaction channel with regard to metastable ion decay (>99%). Second, additional reaction pathways evolve upon collisional activation (CA): complementary eliminations of water and propene are observed in the CA spectra of both *n*-propyl and isopropyl alcohol/Fe^+ complexes. Further, expulsion of a methyl radical takes place in case of *n*-propyl alcohol/Fe^+. This reaction path is not observed in case of the isopropyl alcohol isomer.

As far as dehydration is concerned (Scheme 2), it is well-known that several bare transition-metal cations, after docking at the functional group, can insert easily into the C−O bond of alkanols[35−38] to subsequently liberate neutral H_2O and to form the corresponding

Scheme 2

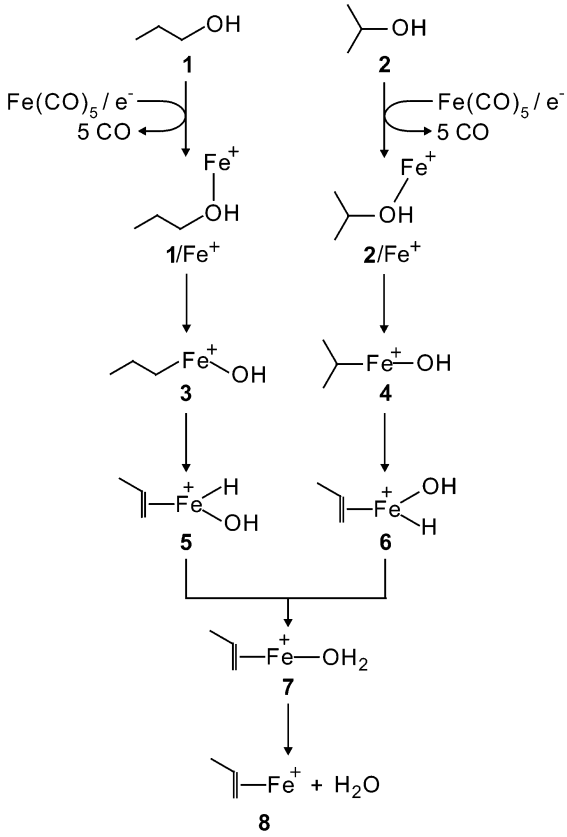

olefin complex of the metal ion via β-hydrogen transfer. Accordingly, our basic mechanistic concept is, that the reactions of *n*-propyl alcohol (**1**) and isopropyl alcohol (**2**) with Fe^+ (or $Fe(CO)_n^+$, $n \leq 5$) initially form the encounter complexes **1**/Fe^+ and **2**/Fe^+, which then can undergo metal insertion to form the intermediates **3** and **4**, respectively. Subsequent β-H transfers to the iron center transform intermediates **3** and **4** to the propene complexes **5** and **6**,[39] respectively, from which reductive elimination gives rise to the bis-ligated complex **7**. The final ionic product $(C_3H_6)Fe^+$ (**8**) originates from loss of water from **7** because propene is more strongly bound to Fe^+ than water; i.e., $D_0(Fe^+-C_3H_6) = 155 \pm 7$ kJ/mol versus $D_0(Fe^+-H_2O) = 129 \pm 7$ kJ/mol.[40] While this scenario involves only a 1,2-elimination mode, 1,1- and 1,3-eliminations are also conceivable for the dehydration. However, it is known from the literature[41] that Fe^+ reacts exclusively via 1,2- and 1,4-eliminations with alkanes, and we assume the same behavior in the case at hand. Since a 1,4-elimination is out of the question for propyl alcohol/Fe^+, we will restrict the mechanistic scenarios to 1,2-eliminations and 1,2-H shifts. In addition, exploratory modeling of the data for 1,*n*-hydrogen shifts with $n \neq 2$ indicates that these reactions do not play a role in the present systems (see below).

Let us begin with a discussion of the MI spectra of the [D_7]-propyl isomers **1i**/Fe^+ and **2g**/Fe^+. Both show almost exclusive losses of HDO, indicating that the

(35) Prüsse, T.; Schwarz, H. *Organometallics* **1989**, *8*, 2856.
(36) Prüsse, T. Ph.D. Thesis, Technische Universität Berlin, D83, 1991.
(37) Karrass, S. Ph.D. Thesis, Technische Universität Berlin, D83, 1994.
(38) Wesendrup, R.; Schalley, C. A.; Schröder, D.; Schwarz, H. *Organometallics* **1996**, *15*, 1435.

(39) The distinction of **5** and **6** is made at this point, because these two structures indeed correspond to two discrete minima, as shown below.
(40) Schröder, D.; Schwarz, H. *J. Organomet. Chem.* **1995**, *504*, 123.
(41) (a) Houriet, R.; Halle, L. F.; Beauchamp, J. L. *Organometallics* **1983**, *2*, 1818 (b) Tolbert, M. A.; Beauchamp, J. L. *J. Am. Chem. Soc.* **1986**, *108*, 7509.

Table 1. Isotopic Distributions for Losses of H_2O and HDO in the MI Mass Spectra of the Deuterated Propyl Alcohol/Fe^+ Complexes[a]

n-propyl alcohols				isopropyl alcohols			
	# D[b]	$-H_2O$	$-HDO$		# D[b]	$-H_2O$	$-HDO$
1a/Fe^+	1	<2.0[c]	>98.0	**2a**/Fe^+	1	<1.0[d]	>99.0
1b/Fe^+	2	82.6	17.4	**2b**/Fe^+	1	94.9	5.1
1c/Fe^+	2	79.5	20.5	**2c**/Fe^+	3	73.4	26.6
1d/Fe^+	2	89.1	10.9	**2d**/Fe^+	3	77.1	22.9
1e/Fe^+	2	85.4	14.6	**2e**/Fe^+	4	58.6	41.4
1f/Fe^+	3	75.0	25.0	**2f**/Fe^+	6	14.9	85.1
1g/Fe^+	3	81.2	18.8	**2g**/Fe^+	7	<0.7	>99.3[e]
1h/Fe^+	5	50.3	49.7				
1i/Fe^+	7	<0.4	>99.6[f]				

[a] Averaged intensities are obtained in three independent experiments normalized to $\sum = 100$. The experimental error is less than ±0.8. In none of these cases has loss of D_2O been observed. [b] Number of D atoms per molecule. [c] Upper limit of H_2O loss derived from analysis of the MI spectra of **1a**/Fe^+ at various degrees of O-deuteration (due to H/D exchange in the inlet system). [d] Upper limit of H_2O loss derived from analysis of the MI spectra of **2a**/Fe^+ at various degrees of O-deuteration (due to exchange in the inlet system). [e] Lower limit of HDO loss derived from analysis of the noise level in the MI spectra of **2g**/Fe^+. [f] Lower limit of HDO loss derived from analysis of the noise level in the MI spectra of **1i**/Fe^+.

Table 2. CA Spectra of the *n*-Propyl Alcohol/Fe^+ Complexes[a]

	possible combinations of lost neutral molecules	**1a**	**1b**	**1c**	**1e**	**1f**	**1g**	**1h**	**1i**
$[M^+ - 15]$	CH_3	6	6	5					
$[M^+ - 16]$	CH_2D				5	3			
$[M^+ - 18]$	CD_3/H_2O		70	70	76	70	77	48	2
$[M^+ - 19]$	HDO	85	17	17	14	24	18	47	95
$[M^+ - 42]$	C_3H_6	2							
$[M^+ - 43]$	C_3H_5D/C_3H_7	3	<1		<1				
$[M^+ - 44]$	$C_3H_4D_2/C_3H_6D$		<1	1	1		<1		
$[M^+ - 45]$	$C_3H_3D_3/C_3H_5D_2$		3	3	2	<1	1		
$[M^+ - 46]$	$C_3H_2D_4/C_3H_4D_3$					1	2	<1	
$[M^+ - 47]$	$C_3HD_5/C_3H_3D_4$							<1	
$[M^+ - 48]$	$C_3D_6/C_3H_2D_5$							2	<1
$[M^+ - 49]$	C_3HD_6								<1
$[M^+ - 50]$	C_3D_7								1
$[M^+ - L]$	*n*-propyl alcohol	4	3	3	2	1	2	2	1

[a] Intensities are normalized to $\sum = 100$.

Table 3. CA Spectra of the Isopropyl Alcohol/Fe^+ Complexes[a]

	possible combinations of lost neutral molecules	**2a**	**2b**	**2c**	**2d**	**2e**	**2f**	**2g**
$[M - 18]$	H_2O	92	81	57	66	41	11	
$[M - 19]$	HDO	2	4	28	21	42	78	89
$[M - 42]$	C_3H_6	2						
$[M - 43]$	C_3H_5D/C_3H_7	2	7					
$[M - 44]$	$C_3H_4D_2/C_3H_6D$		4	2	1			
$[M - 45]$	$C_3H_3D_3/C_3H_5D_2$			4	4	4		
$[M - 46]$	$C_3H_2D_4/C_3H_4D_3$			4	4	2		
$[M - 47]$	$C_3HD_5/C_3H_3D_4$				<1	4	4	
$[M - 48]$	$C_3D_6/C_3H_2D_5$						<1	5
$[M - 49]$	C_3HD_6					1	3	
$[M - 50]$	C_3D_7							2
$[M - L]$	isopropyl alcohol	2	4	5	4	4	4	4

[a] Intensities are normalized to $\sum = 100$.

intact hydroxyl group is present in the eliminated water molecule (Table 1). Elimination of D_2O is not observed; instead, there are traces of H_2O losses which can be attributed to incomplete deuteration of the propyl alcohols (>98 atom % D) and originate from the interference of isobaric [^{13}C][D_6]-propyl alcohol/Fe^+. Similar effects are seen for **1a**/Fe^+ and **2a**/Fe^+, where HDO formation clearly dominates (>98%), and the minor amount of H_2O eliminations (<2%) is ascribed to H/D exchanges of the OD group occurring within the mass spectrometer, which cannot be suppressed completely.[42]

The labeling data of the remaining isotopomers reveal extensive H/D equilibrations in the course of water loss. In particular, the observed H_2O/HDO ratios clearly rule out the exclusive occurrence of selective 1,2-eliminations. In the case of **1b**/Fe^+, for example, one would expect a specific loss of H_2O, if only a 1,2-elimination were operative. The fact that 17.4% of the water eliminated corresponds to HDO demonstrates that H/D exchange within the alkyl group has taken place. Similar conclusions can be inferred from the isopropyl alcohol/Fe^+ complexes. Thus, a direct 1,2-elimination from **2f**/Fe^+ should give rise to exclusive loss of HDO, whereas the experimentally observed formation of 14.9% H_2O clearly indicates partial H/D equilibration. Interestingly, however, a more careful comparison of those isotopomers having the same number of deuterium atoms suggests that, to some extent, a selective 1,2-eliminination is still operative. Let us take the set of [D_2] isotopomers of *n*-propyl alcohol as an example: the H_2O/HDO ratios vary from 79.5/20.5 (**1c**/Fe^+) to 89.1/10.9 (**1d**/Fe^+). Thus, clearly beyond the experimental error margins, the initial positions of the H and D atoms in the alkyl backbone still influence the isotope distributions to a notable degree. Another interesting point can likewise be seen by comparing the Fe^+ complexes of *n*-propyl and isopropyl alcohols having the same deuterium content, thereby underlining some differences between both isomers even though they (i) eventually lead to identical products and (ii) quite obviously undergo H/D equilibration along the reaction path. **1g**/Fe^+ and **2c**/Fe^+, for example, show distinctly different H_2O/HDO ratios (81.2/18.8 and 73.4/26.6, respectively), and similarly, though less pronounced, a significant difference is observed for the couple **1f**/Fe^+ and **2d**/Fe^+ (Table 1). It remains to be noted that the comparison of **1b**/Fe^+ (H_2O/HDO = 82.6/17.4) and **1h**/Fe^+ (H_2O/HDO = 50.3/49.7) indicates that loss of water is associated with a notable kinetic isotope effect (KIE), because reciprocal H_2O/HDO ratios are to be expected otherwise, due to the inverse deuteration patterns. Similar conclusions apply for the H_2O/HDO ratios of the Fe^+ complexes of **2b**,**f**.

In the CA spectra, $(H_2O)Fe^+$ and $(C_2H_4)FeOH^+$ occur as additional ionic products (Tables 2 and 3). The appearance of new product channels can be attributed to the fact that the system gains more internal energy upon CA, such that energetically more demanding routes become accessible. Accordingly, the observation of $(H_2O)Fe^+$ as an ionic fragment in the CA spectra is consistent with loss of the more strongly bound propene ligand from the bis-ligated complex **7**. While the *n*-propyl and isopropyl isomers both lose water and propene, quite interestingly, C−C bond cleavage result-

(42) Due to H/D exchange of the OD group with the tube walls of the mass spectrometer, a certain amount of unlabeled **1**/Fe^+ is also present in the ion source. When the ions of interest (**1a**/Fe^+) are mass-selected, an interference of the ^{13}C peak of **1**/Fe^+, which has the same nominal mass as **1a**/Fe^+, cannot be prevented. [$^{13}C_1$]-**1**/Fe^+ can, of course, only lose H_2O, and this interference accounts for the observed H_2O loss.

ing in the expulsion of a methyl radical is only observed in the case of the *n*-propyl alcohol/Fe^+ complexes. This finding readily implies that the isomerization of *n*-propyl alcohol/Fe^+ and isopropyl alcohol/Fe^+ is associated with a barrier. While the energies deposited in high-energy CA experiments are likely to surmount this barrier and to bring about both interconversion and dissociation via direct C−C bond cleavage, it is the entropically more favored dissociation path which is preferably populated immediately after the collision. As outlined previously at great length,[43] different CA mass spectra imply that isomeric ions—prior to the collision experiment—have not undergone complete interconversion.

With respect to the suggestion that the metastable complexes of **1**/Fe^+ and **2**/Fe^+ merge in structure **7** (Scheme 2) while retaining the structural integrity of the hydroxyl group, it is therefore implied that at least one of the reaction steps connecting *n*-propyl alcohol/Fe^+ and isopropyl alcohol/Fe^+ must be irreversible. As the hydroxyl group remains intact over the course of dehydration (Table 1), the steps **5** → **7** and **6** → **7** must be irreversible. The fact that extensive H/D equilibration of the alkyl chain is observed implies that **3** → **5** and **4** → **6** are reversible processes. To allow for scrambling, **3** and **5** must be reversibly interconvertible with **4** and **6**. This is granted by **TS 5/6**: namely, a rotation around the Fe−propene axis. Which of the steps precisely corresponds to the kinetic bottleneck cannot be deduced on the basis of the labeling data; however, as will be shown later according to the computational findings, it is the insertion of Fe^+ into the C−O bond, i.e., **1** → **3** and **2** → **4**, which is highest in energy demand. This hypothesis is further corroborated by the finding that methyl-radical loss from **1**/Fe^+ and its isotopomers occurs without any significant isotopic scrambling (see Table 2).

Another interesting observation evolves from the comparison of the isotope distributions for water losses in the MI and CA spectra. Generally, the corresponding H_2O/HDO ratios are rather similar to each other (e.g., 81.2/18.8 (MI) and 81.8/18.2 (CA) for **1g**/Fe^+ or 77.1/22.9 (MI) and 76.1/23.9 (CA) for **2d**/Fe^+). Note that part of the similarity of the MI and CA spectra in the present experiments is due to the extremely long field-free region in the Berlin four-sector instrument. Thus, metastable-ion decomposition can occur along a flight path of about 1.9 m, whereas collisional activation is confined to only 10 cm of the flight path at most. Therefore, the CA spectra are superimposed with a substantial MI fraction for the more easily dissociating propyl alcohol/Fe^+ complexes. Notwithstanding, in some cases the differences between the MI and CA spectra are more distinct. For example, the amount of HDO increases from 26.6% in the MI spectra to 33.0% upon collisional activation in the case of **2c**/Fe^+. Quite likely, these findings point to the operation of a subtle interplay between internal energies and position-dependent kinetic isotope effects. Isotopically sensitive branching, operative in organometallic chemistry and other fields, has been reported repeatedly.[44−47]

The experimental data in Table 1 contain even more valuable information than apparent in the preceding

Scheme 3

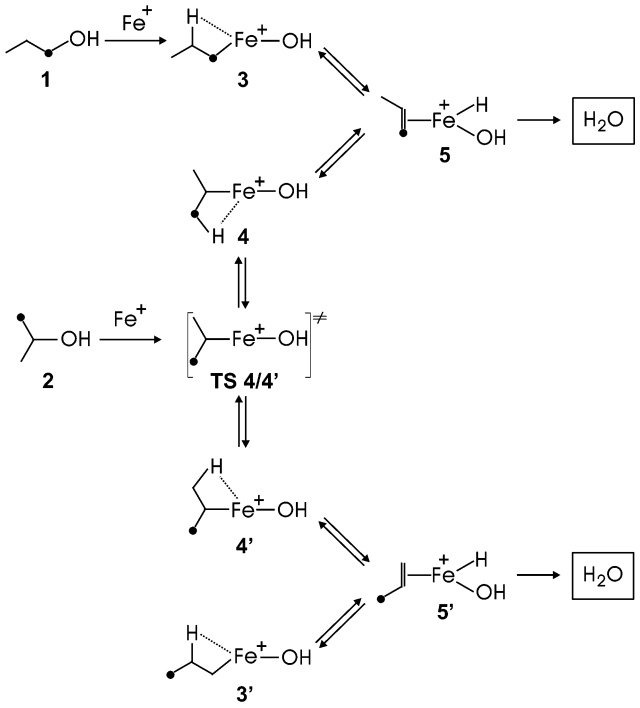

exploratory analysis. Consider the MI spectra of the [D_2]-*n*-propyl alcohol complexes **1b**/Fe^+, **1c**/Fe^+, **1d**/Fe^+, and **1e**/Fe^+. The H_2O/HDO ratios for **1b**/Fe^+ (82.6/17.4) and **1c**/Fe^+ (79.5/20.5) are quite similar, yet not identical, suggesting that—neglecting KIEs for the time being—nearly complete H/D equilibration at C(1)/C(2) occurred. In distinct contrast, **1d**/Fe^+ (89.1/10.9) and **1e**/Fe^+ (85.4/14.6) yield significantly lower amounts of HDO. Actually, it takes a [D_3] isotopomer, **1g**/Fe^+ (81.2/18.8), to achieve H_2O/HDO ratios comparable to that of the [D_2]-labeled complexes **1b**/Fe^+ and **1c**/Fe^+. These findings have profound implications for the mechanistic scenario of the Fe^+-mediated dehydration. Obviously, the four hydrogen atoms attached to C(1) and C(2) of *n*-propyl alcohol are almost completely equilibrated, whereas the terminal methyl group is participating to a lower extent. As equilibration of C(1) and C(2) is traditionally assumed to involve an isopropyl intermediate (e.g., **5** ⇄ **4**), C(1) and C(3) of the *n*-C_3H_7 unit are hence expected to become equivalent. However, this is clearly not the case and, consequently, one is facing a mechanistic dilemma. We have considered various scenarios aimed at resolving this conflicting situation, and the most promising model is shown in Scheme 3. The (newly formed) methyl group generated in the case of *n*-propyl → isopropyl isomerization **3** ⇄ **4**, while constitutionally equivalent with the methyl group already present in the *n*-propyl backbone, remains inherently asymmetric due to the operation of a β-agostic interaction. Consequently, a memory effect reflecting to some extent the history of the isomerization is operative in the isotope distribution of the H_2O/HDO losses.[48] This

(43) For further discussions and references, see: (a) Levsen, K.; Schwarz, H. *Angew. Chem., Int. Ed. Engl.* **1976**, *15*, 509. (b) Levsen, K.; Schwarz, H. *Mass Spectrom. Rev.* **1983**, *2*, 77.

(44) Thibblin, A.; Ahlberg, P. *Chem. Soc. Rev.* **1989**, *18*, 209.

(45) Prüsse, T.; Fiedler, A.; Schwarz, H. *Helv. Chim. Acta* **1991**, *74*, 1127.

(46) Seemeyer, K.; Prüsse, T.; Schwarz, H. *Helv. Chim. Acta* **1993**, *76*, 1632.

(47) Raabe, N.; Karrass, S.; Schwarz, H. *Chem. Ber.* **1994**, *127*, 261.

(48) Trage, C.; Zummack, W.; Schröder, D.; Schwarz, H. *Angew. Chem., Int. Ed.* **2001**, *40*, 2708.

scenario is depicted in Scheme 3, where the C(1) position is deliberately marked by a dot to indicate its "history" in the rearrangement.

The key assumption of this model is that **4** and **4′** are suggested to exist as discrete minima due to stabilization via β-agostic interactions with a hydrogen atom of the incipient methyl group. Consequently, these particular hydrogen atoms are predestined to be activated and transferred to the metal center in the ensuing steps. For *n*-propyl alcohol/Fe^+, this scenario implies that the preferentially observed equilibration of the H/D atoms attached to C(1) and C(2) occurs via **3** and **4**, whereas the H/D atoms at C(3) participate in H/D scrambling, only if **4** interconverts to **4′** via the associated transition structure **TS 4/4′**. The energy demand associated with **TS 4/4′** as well as the internal energy content of the complex will therefore determine the degree of C(1)/C(3) methyl group asymmetry apparent in the experiments. This is as much as a qualitative analysis is able to tell about the dissociation of metastable propyl alcohol/Fe^+ complexes.

4.2. Kinetic Modeling. As noted above, metal-mediated H/D equilibrations observed in many organometallic reactions are described only phenomenologically in most cases, rather than analyzed rigorously, because the interplay of various competing reactions often associated with KIEs appears to be too complex. In this section, a quantitative analysis of the experimentally observed isotope patterns is attempted. The above considerations of the H_2O/HDO ratios already provide some helpful boundary conditions for any kinetic model aimed at describing the propyl alcohol/Fe^+ systems, and the essential findings are briefly recalled here: (i) the hydroxyl moiety remains intact in the course of water loss, (ii) H/D transfer from the propyl backbone is associated with a significant KIE, (iii) *n*-propyl and isopropyl alcohol/Fe^+ behave differently, and (iv) alkyl hydrogen atoms do not equilibrate completely; rather, the isotope distributions indicate a memory effect concerning their origins. Therefore, the simplest model to describe the experimental data has to consider the existence of a net KIE as well as a distinction between scrambling of alkyl hydrogens and a direct selective 1,2-elimination mode.

The general algebraic structure of all kinetic models used in this work is shown in eq 1. Briefly, the

$$\frac{H_2O}{HDO} = \frac{f_s[P_H(\beta)] + (1 - f_s)[P_H(\text{alkyl})]}{f_s[P_D(\beta)] + (1 - f_s)[P_D(\text{alkyl})]}\,\text{KIE} \quad (1)$$

H_2O/HDO ratios are modeled by a quotient in which the terms given in the numerator represent the two different ways to lose H_2O, i.e., selective 1,2-elimination vs H_2O loss after complete alkyl H/D equilibration, and the terms in the denominator are defined accordingly for the elimination of HDO. The first addend of the numerator describes the fraction of the molecules that react via a direct, selective 1,2-elimination (f_s) of H_2O multiplied by the probability to actually find an H atom in a position β to the Fe atom ($P_H(\beta)$). Accordingly, the fraction of the complexes that eliminate H_2O after complete alkyl H/D equilibration, $1 - f_s$, multiplied by the probability of finding an H atom at any position of the alkyl chain (P_H(alkyl)), comprises the second addend. In the denominator, the HDO losses are described in an analogous fashion.

Table 4. H_2O and HDO Losses from Metastable Complexes of Fe^+ with Labeled Isopropyl Alcohols

	exptl		model A[a]		model B[b]	
	$-H_2O$	$-$HDO	$-H_2O$	$-$HDO	$-H_2O$	$-$HDO
2a/Fe^+	<1.0[c]	>99.0	0.0	100.0	0.0	100.0
2b/Fe^+	94.9	5.1	95.4	4.6	94.9	5.1
2c/Fe^+	73.4	26.6	70.7	29.3	73.0	27.0
2d/Fe^+	77.1	22.9	75.8	24.2	77.3	22.7
2e/Fe^+	58.6	41.4	56.6	43.4	59.0	41.0
2f/Fe^+	14.9	85.1	16.4	83.6	14.9	85.1
2g/Fe^+	<0.7	>99.3[d]	0.0	100.0	0.0	100.0
MAD[e]			4.7		0.4	
MD[f]			10.0		0.9	

[a] Parameters: $f_s = 0.38$ and KIE = 2.02. [b] Parameters: $f_s = 0.52 \pm 0.02$, $KIE_s = 5.2 \pm 0.4$, and $KIE_x = 1.40 \pm 0.03$. [c] Upper limit of H_2O loss derived from the analysis of the MI spectra of **2a** at various degrees of O-deuteration (due to H/D exchange in the inlet system). [d] Lower limit of HDO loss derived from analysis of the noise level in the MI spectra of **2g**/Fe^+. [e] Mean absolute deviation (in percent) from the experimental results. [f] Maximum deviation (in percent) from the experimental results.

In the following, this general expression of the kinetic model is applied to the *n*-propyl alcohol/Fe^+ and isopropyl alcohol/Fe^+ systems. Because the isopropyl system is more simple due to the constitutional equivalence of the methyl groups, the isopropyl alcohol/Fe^+ complexes are discussed first. The most simple approach (model A) includes only two parameters: (i) a selective 1,2-elimination (f_s)—which also defines the fraction of water elimination after complete H/D equilibration ($1 - f_s$)—and (ii) an averaged kinetic isotope effect (KIE). Accordingly, the data of the isotopologous **2**/Fe^+ complexes can thus be described by eq 2 (model A).

$$\frac{H_2O}{HDO} = \frac{f_s\frac{1}{6}\left(6 - \sum_{i=2}^{7} x_i\right) + (1 - f_s)\frac{1}{7}\left(7 - \sum_{x=1}^{7} x_i\right)}{f_s\frac{1}{6}\sum_{i=2}^{7} x_i + (1 - f_s)\frac{1}{7}\sum_{i=2}^{7} x_i}\,\text{KIE} \quad (2)$$

While model A already reproduces the experimental data reasonably well (Table 4), some significant discrepancies remain. Therefore, the refined model B (eq 3) was developed in which the net KIE is split into KIE_s and KIE_x, accounting for the possibility that the kinetic isotope effects associated with the selective 1,2-elimination (KIE_s) and the scrambling (KIE_x) differ from each other.

$$\frac{H_2O}{HDO} = \frac{f_s\frac{1}{6}\left(6 - \sum_{i=2}^{7} x_i\right) + (1 - f_s)\frac{1}{7}\left(7 - \sum_{i=1}^{7} x_i\right)}{\frac{f_s}{KIE_s} \times \frac{1}{6}\sum_{i=2}^{7} x_i + \frac{1 - f_s}{KIE_x} \times \frac{1}{7}\sum_{i=1}^{7} x_i} \quad (3)$$

Despite its simplicity, model B provides excellent agreement with the experimental findings for the isopropyl alcohol/Fe^+ system (Table 4). The best fit is obtained with $f_s = 0.52 \pm 0.04$, $KIE_s = 5.2 \pm 0.4$, and $KIE_x = 1.40 \pm 0.03$. For the unlabeled system, these parameters imply more or less equal amounts of selec-

Table 5. H_2O and HDO Losses from Metastable Complexes of Fe^+ with Labeled *n*-Propyl Alcohols

	exptl		model B[a]		model C[b]	
	$-H_2O$	$-HDO$	$-H_2O$	$-HDO$	$-H_2O$	$-HDO$
1a/Fe^+	<2.0[c]	>98.0	0.0	100.0	0.0	100.0
1b/Fe^+	82.6	17.4	86.4	13.6	83.0	17.0
1c/Fe^+	79.5	20.5	81.3	18.7	80.3	19.7
1d/Fe^+	89.1	10.9	86.4	13.6	88.8	11.2
1e/Fe^+	85.4	14.6	83.7	16.3	84.8	15.2
1f/Fe^+	75.0	25.0	74.6	25.4	73.7	26.6
1g/Fe^+	81.2	18.8	77.0	23.0	82.0	18.0
1h/Fe^+	50.3	49.7	46.8	53.2	50.3	49.7
1i/Fe^+	<0.4	>99.6[d]	0.0	100.0	0.0	100.0
MAD[e]			3.5		0.7	
MD[f]			7.0		1.7	

[a] Parameters: $f_{sH} = -0.033$, $KIE_s = -0.557$, and $KIE_x = 2.667$. [b] Parameters: $f_s = 0.068 \pm 0.003$, $KIE_s = 6.1 \pm 0.5$, $KIE_x = 2.149 \pm 0.005$, and $c_{as} = 0.697 \pm 0.004$. [c] Upper limit of H_2O loss derived from analysis of the MI spectra of **1a**/Fe^+ at various degrees of O-deuteration (due to H/D exchange in the inlet system). [d] Lower limit of HDO loss derived from analysis of the noise level in the MI spectra of **1i**/Fe^+. [e] Mean absolute deviation (in percent) from the experimental results. [f] Maximum deviation (in percent) from the experimental results.

tive 1,2-elimination (52%) and complete equilibration prior to loss of water (48%).[49]

In contrast, application of model B to the *n*-propyl alcohol/Fe^+ system (eq 4) gives rather poor agreement between experimental and modeled data (Table 5), and even more important, some of the parameters are physically unrealistic: e.g., $f_s < 0$ and $KIE_s < 0$.

$$\frac{H_2O}{HDO} = \frac{f_s \frac{1}{2}\left(2 - \sum_3^4 x_i\right) + (1 - f_s)\frac{1}{7}\left(7 - \sum_1^7 x_i\right)}{\frac{f_s}{KIE_s} \times \frac{1}{2}\sum_{i=3}^4 x_i + \frac{1 - f_s}{KIE_x}\frac{1}{7} \times \sum_{i=1}^7 x_i} \quad (4)$$

Quite clearly, assuming a simple sequence of C−O bond insertion and subsequent β-hydrogen shifts does not suffice for a quantitative description of the **1**/Fe^+ system. This is not only reflected in the poor agreement between modeled and experimental data but also indicated in the qualitative analysis, in which a distinction between the four hydrogen atoms bound to C(1) and C(2) and those at C(3) has to be taken into account. Therefore, another parameter is necessary to model the *n*-propyl alcohol/Fe^+ data. To this end, the asymmetry term c_{as} is introduced (model C), which constrains the involvement of the methyl group comprising the original position C(3) in the dehydration (eq 5).

The asymmetry factor, c_{as}, has to fulfill two boundary conditions. In case there is no preference of one methyl group over the other ($c_{as} = 1$), the part accounting for H/D scrambling has to reflect the scrambling of the seven hydrogen atoms involved. If the asymmetry is complete ($c_{as} = 0$), that is, the hydrogen transfer exclusively involves the hydrogens attached to C(1) and C(2), the model has to reflect the scrambling of only these four hydrogen atoms. This is achieved by separating P_H(alkyl) into P_H(C(1) + C(2)) and $c_{as}[P_H(C(3))]$. An analogous procedure is applied to define P_D(alkyl). Equation 5 meets these requirements and is able to fit the experimental data reasonably well (Table 5). We note in passing that model B for **2**/Fe^+ and model C for **1**/Fe^+ do not differ fundamentally. For the isopropyl alcohol/Fe^+ complexes, by definition, the asymmetry factor $c_{as} = 1$, as the methyl groups in substrate **2** are identical. Hence, for **2**/Fe^+ and its isotopologues model C simplifies to model B.

$$\frac{H_2O}{HDO} = \frac{f_s \frac{1}{2}\left(2 - \sum_{i=3}^4 x_i\right) + (1 - f_s)\frac{1}{4 + 3c_{as}}\left[4 - \sum_{i=1}^4 x_i + c_{as}\left(3 - \sum_{i=5}^7 x_i\right)\right]}{\frac{f_s}{KIE_s} \times \frac{1}{2}\sum_{i=3}^4 x_i + \frac{1 - f_s}{KIE_x} \times \frac{1}{4 + 3c_{as}}\left[\sum_{i=1}^4 x_i + c_{as}\sum_{i=5}^7 x_i\right]} \quad (5)$$

For the *n*-propyl alcohol/Fe^+ system, the best fit of model C is obtained for $f_s = 0.068 \pm 0.003$, $KIE_s = 6.1 \pm 0.5$, $KIE_x = 2.149 \pm 0.005$, and $c_{as} = 0.697 \pm 0.004$. In comparison, the amount of a selective, direct 1,2-elimination mode is much lower for *n*-propyl alcohol/Fe^+ than for isopropyl alcohol/Fe^+ complexes, in that only about 7% of selective dehydration occurs for **1**/Fe^+ compared to 52% for **2**/Fe^+. While the experiments clearly demonstrate an asymmetry between the already existing and the newly formed methyl group in the isomerization **3** ⇄ **4**, the chemical origin of this effect remains unresolved. For this reason, relevant parts of the potential-energy surface were explored by computational means, as described next.

4.3. Computational Findings. Quantum-chemical calculations were carried out to elucidate the reaction profiles of Fe^+ with *n*-propyl and isopropyl alcohol, yielding $(C_3H_6)Fe^+$ (**8**) and water on three spin surfaces. At the B3LYP/DZP level, the quartet surface is the energetically most favored one throughout the reaction coordinates (Figures 1 and 2). Due to their higher energy demands, we will not pursue the doublet and sextet states any further and rather focus on the description of the quartet surface.

Relative energies are obtained as B3LYP/TZP and *m*PW1PW91/TZP single-point calculations using the structures optimized at the B3LYP/DZP level. The major difference between the *m*PW1PW91 and B3LYP results concerns the description of the bare Fe^+ cation. Thus, the B3LYP/TZP splitting of 0.1 kJ/mol deviates significantly from the experimental sextet/quartet splitting (23.9 kJ/mol[31]), while the splitting of 17 kJ/mol predicted at the *m*PW1PW91/TZP level of theory is in much better agreement with the spectroscopic value. The difference of the two methods in describing the atomic Fe^+ is also reflected in the ligated species **1**/Fe^+, **2**/Fe^+, **3**, **4**, and **8**. Preliminary calculations[34] demonstrate that the *m*PW1PW91 energies are roughly shifted upward by 30−40 kJ/mol compared to the B3LYP results for all structures relative to the entrance channel (Fe^+ and propyl alcohol). Moreover, compared to B3LYP, *m*PW1PW91 is supposedly superior in describing weak interactions,[27] such as agostic bonding, which is relevant in this case. Accordingly, we restrict ourselves to the *m*PW1PW91/TZP//B3LYP/DZP results.

(49) Note that the KIEs obtained by this modeling procedure do not correspond to intrinsic but apparent isotope effects which inherently comprehend the competition of the various pathways. For details, see ref 44 and arguments outlined there.

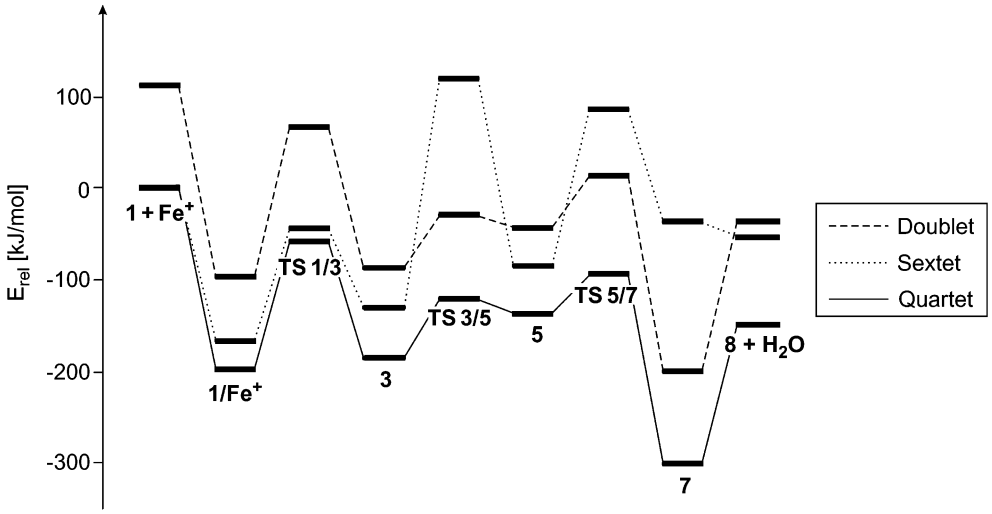

Figure 1. Quartet, doublet, and sextet spin surfaces for the reaction of Fe^+ with *n*-propyl alcohol **1** (B3LYP/DZP).

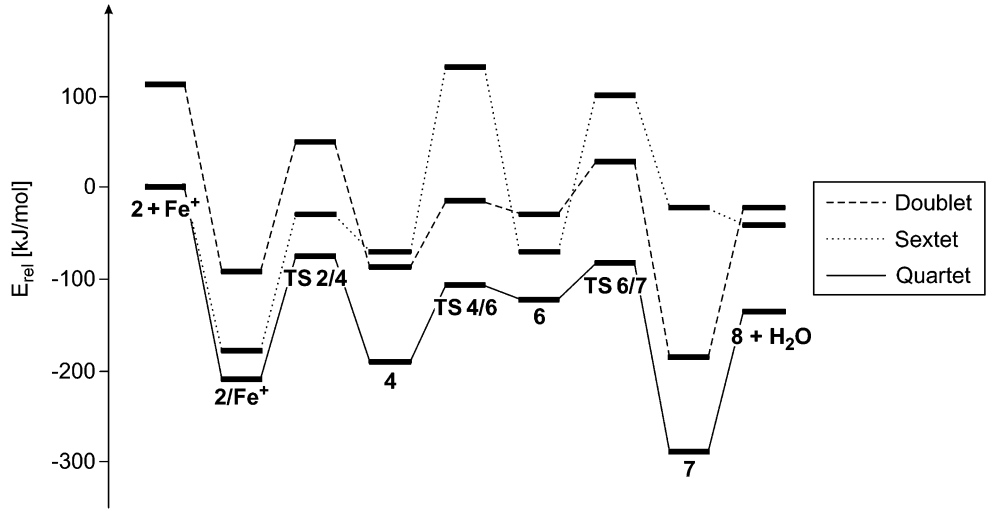

Figure 2. Quartet, doublet, and sextet spin surfaces for the reaction of Fe^+ with isopropyl alcohol **2** (B3LYP/DZP).

At first, let us briefly comment upon the overall energetics before describing the various mechanistic details. The reaction of Fe^+ and isopropyl alcohol to form water and cationic propene/Fe^+ (**8**) is calculated to be exothermic by 135 kJ/mol (experimental 100.8 kJ/mol[50]). The calculations of the analogous reaction with *n*-propyl alcohol predict an exothermicity of 149 kJ/mol (experimental 118.5 kJ/mol[50]). The slight overestimation of the computed reaction enthalpy can be ascribed to the well-known "overbinding" of $Fe(C_3H_6)^+$ compared to Fe^+ and C_3H_6, which is common for DFT methods.[8] Further note that both reactions are not energetically hindered, because all minima and transition structures of the quartet surface are located below the corresponding entrance channels: i.e., bare Fe^+ and **1** or **2**, respectively.

The reaction pathways shown in Figure 3 commence with the formation of the corresponding encounter complexes. **1**/Fe^+ consists of an essentially unperturbed *n*-propyl alcohol structure with the metal cation coordinating to the oxygen at a distance of 198 pm (Chart 3). As a result of ion/dipole interaction, the C−O bond is slightly elongated by 4 pm. Likewise, **2**/Fe^+ consists of a by and large unperturbed isopropyl alcohol ligand which interacts with Fe^+ via coordination to the oxygen atom. Again, the C−O bond in **2**/Fe^+ is 8 pm longer than in free isopropyl alcohol and additionally both adjacent C−C bonds are shortened slightly by 1 pm. The barrier for the insertion of the metal cation into the C−O bond is the energetically most demanding step en route to propene/Fe^+ (**8**) and water with −19 and −56 kJ/mol for **TS 1/3** and **TS 2/4**, respectively. Apart from the expected elongations of the C−O bonds, the insertions of Fe^+ are accompanied by further shortenings of the adjacent C−C bonds by 4 pm in both **TS 1/3** and **TS 2/4** (Chart 4). The resulting insertion intermediates **3** and **4** are characterized by one particularly short Fe−β-H bond (190 and 193 pm for **3** and **4**, respectively), clearly indicating their stabilization by agostic interactions. The Fe−C and Fe−O distances in **3** and **4** are consistent with the formation of two covalent bonds in each of the insertion intermediates. Note that the C−C bonds which are shortened in **TS 1/3** and **TS 2/4** are relaxed approximately to their lengths in the corresponding encounter complexes. Due to the agostic interaction in structure **4**, the iron is not located symmetrically between C(1) and C(3) but shifted toward

(50) Lias, S. G.; Bartmess, J. E.; Liebmann, J. F.; Holmes, J. L.; Levin, R. D.; Mallard, W. G. *J. Phys. Chem. Ref. Data* **1988**, *17*, Supplement No. 1. URL: http://physics.nist.gov/PhysRefData/.

Chart 3

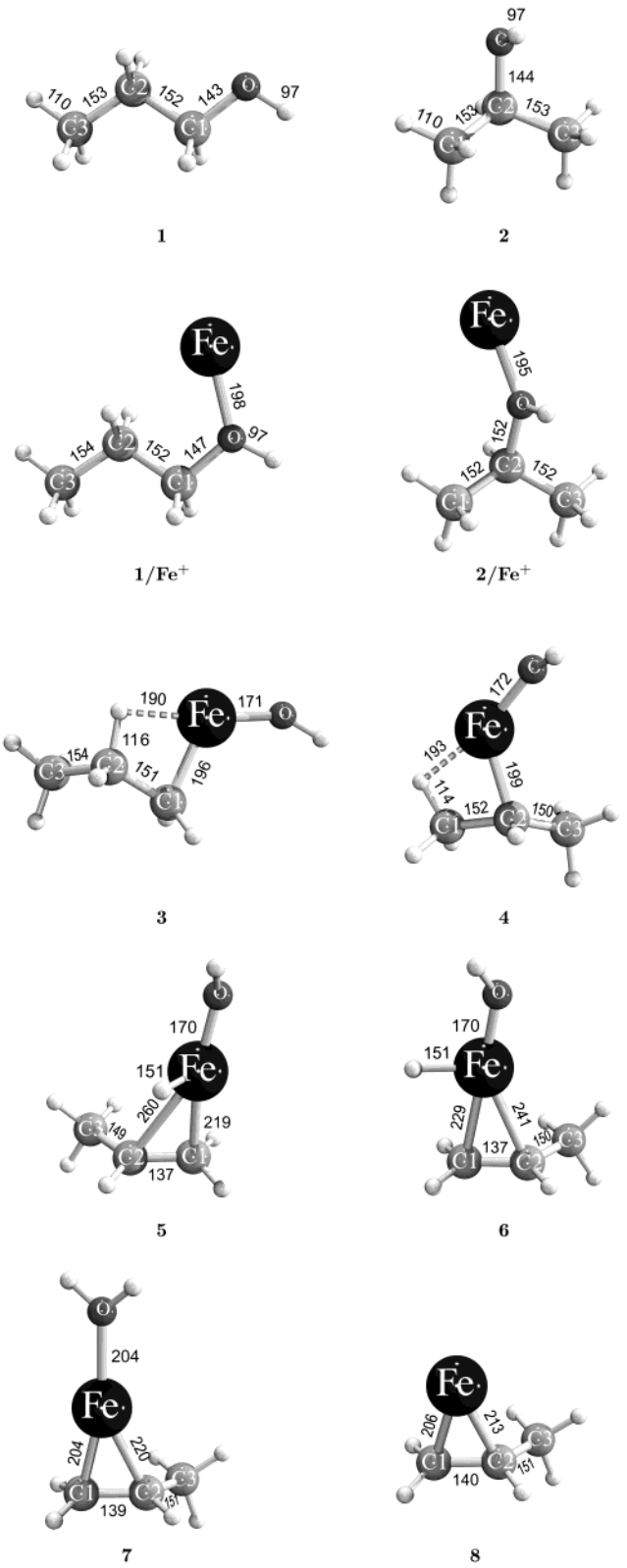

Chart 4

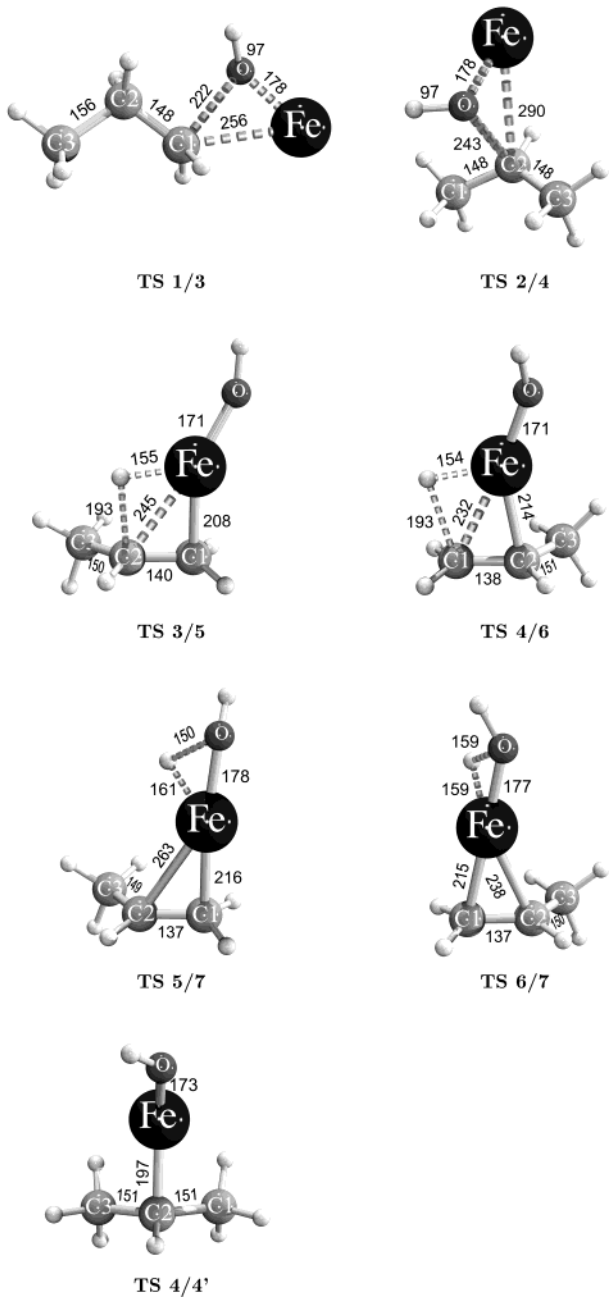

one carbon atom, in that the C(1)C(2)Fe angle of 81° is notably smaller than the corresponding C(3)C(2)Fe angle of 113°. As a next step, we consider β-hydrogen transfer from the propyl units to the metal cation.[51,52]

TS 3/5 and **TS 4/6** associated with β-H migration can be described as late transition structures with geometries similar to those of the emerging complexes **5** and **6**; i.e., the relevant Fe−H distances amount to 155 pm in **TS 3/5** and 154 pm in **TS 4/6** compared to 151 pm in **5** as well as **6**. The C−C bonds in **5** and **6** are shortened significantly to 137 pm, indicating the formation of propene, which is further supported by a gradual planarization of the respective olefinic C atoms. Notably, the metal atom in **5** is located fairly asymmetrically between the two carbon atoms of the propene ligand

(51) Attempts to model the experimental data by involving 1,1- and 1,3-H shifts did not only lead to a poor consistency between experimental and modeled data but, more importantly, also resulted in physically meaningless parameters.

(52) Further, we note in passing that, on the basis of computational studies, in the reactions of Fe^+ with small hydrocarbons C−H and C−C bond activation involves multicenter intermediates. For leading references on this topic which, however, has not been adressed in the present work, see: (a) Holthausen, M.; Fiedler, A.; Schwarz, H.; Koch, W. *J. Phys. Chem.* **1996**, *100*, 6236. (b) Yi, S. S.; Reichert, E. L.; Holthausen, M. C.; Koch, W.; Weisshaar, J. C. *Chem. Eur. J.* **2000**, *6*, 2232.

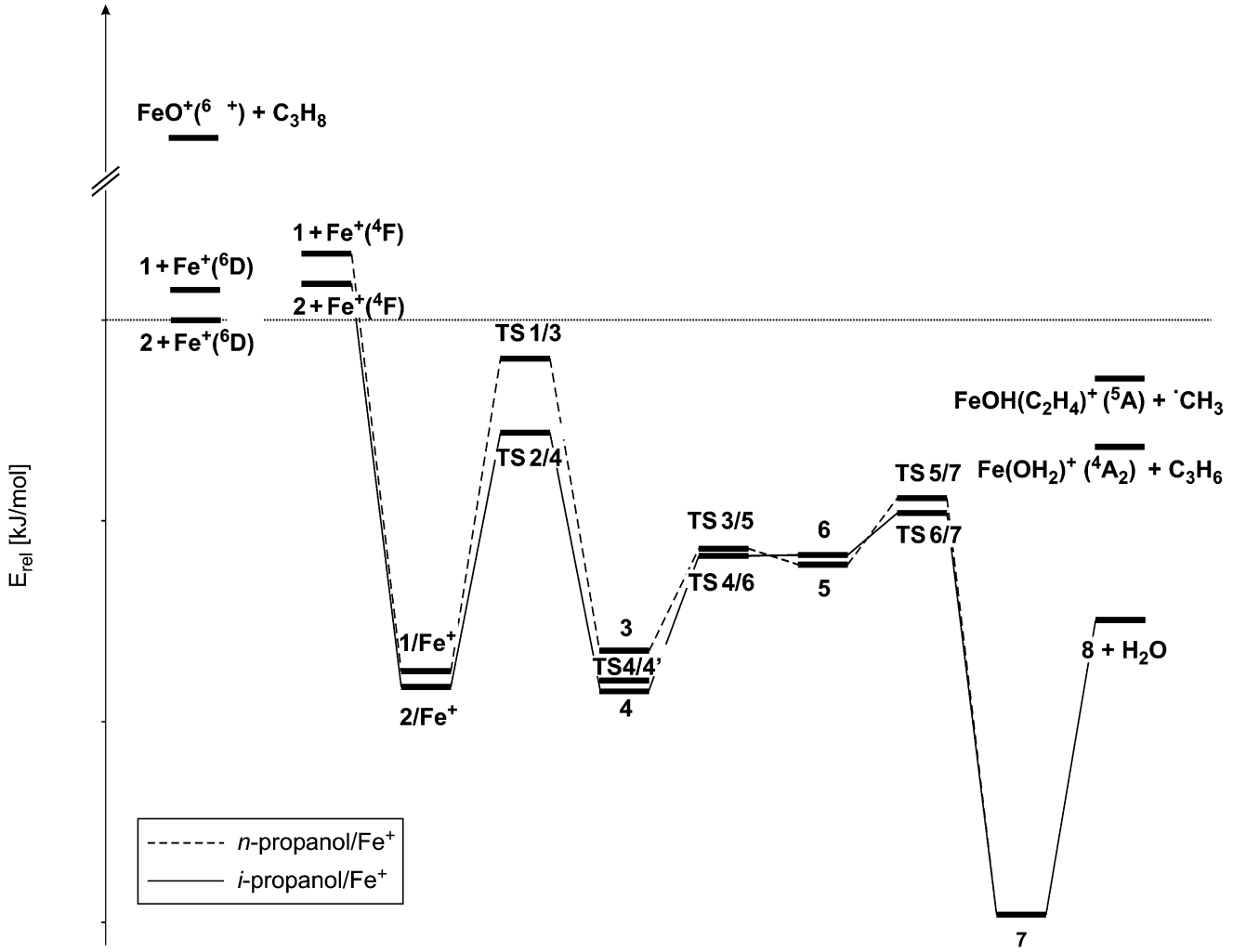

Figure 3. Quartet PES for the reaction of Fe^+ with *n*-propyl and isopropyl alcohol, yielding $(C_3H_6)/Fe^+$ (**8**) and H_2O (*m*PW1PW91/TZP//B3LYP/DZP with ZPVE correction). The dotted horizontal line represents the relative energy of the separated ground-state species **2** and $Fe^+(^6D)$. Additionally, energies for the entrance and exit channels of the FeO^+/C_3H_8 system are given to allow for a better comparison of the three isomeric systems (see text for details).

($r_{Fe-C(1)}$ = 219 pm and $r_{Fe-C(2)}$ = 260 pm). This asymmetry is much less pronounced in **6**, where the analogous Fe−C bonds differ only by 12 pm. Structures **5** and **6** reside in quite shallow wells on the PES. As **TS 5/7** corresponds to the highest point in either direction of the reaction coordinates for **5** (and **6**), no barriers larger than 33 kJ/mol exist. **5** and **6** can be interconverted by a formal rotation around the Fe−propene axis (**TS 5/6**). On the basis of a single-point calculation, the barrier for this rotation amounts to approximately 3 kJ/mol.[53] Finally, 1,2-H shifts from Fe to O (**TS 5/7** and **TS 6/7**, respectively) lead to the bis-ligated complex **7**, in which the reaction pathways of isopropyl and *n*-propyl alcohol have finally merged in a common structure. While the Fe atom is still not located symmetrically between C(1) and C(2) in **7**, the Fe−C distances have shortened, thus indicating a stronger Fe−propene interaction. This is also reflected in the slightly elongated C−C double bond of **7**, which is 2 pm longer than in **5** and **6**, respectively. The Fe−O bond is also stretched to 204 pm, indicating an ion/dipole interaction between water and the propene/Fe^+ unit. From **7**, the exit channel to produce $Fe(C_3H_6)^+$ (**8**) is reached by simple evaporation of the water ligand (Figure 3).As far as the reversibility of each of the suggested reaction steps is concerned, one of the crucial experimental findings is the nonparticipation of the OH group in the hydrogen atom scrambling. This observation is in good agreement with the theoretical results. Once **7** is formed via a 1,2-H shift, the barrier for the reverse reaction is 53 kJ/mol larger than the energy required for loss of the coordinated water molecule to generate **8**. Moreover, dissociation of **7** is kinetically favored by the fact that the density of states is larger for a simple bond cleavage than for the intramolecular rearrangement via a 1,2-H shift. Next, the computed reaction profiles suggest that the insertions of Fe^+ into the C−O bonds of **1** and **2** constitute the rate-determining steps, which is also in agreement with the experimental data. Furthermore, it is worth noting that the insertion barriers represent the largest energetic difference in comparison of the potential-energy surfaces of the *n*-propyl and isopropyl alcohol complexes in that **TS 1/3** is 37 kJ/mol more energy demanding than **TS 2/4**. As a consequence, *n*-propyl alcohol complexes entering the system via **TS 1/3** will

(53) The actual transition structure could not be located because geometry optimizations always yielded transition structures for rotation of the methyl group or for a 1,2-H shift from Fe to O. Hence, the barrier height was estimated from a relaxed potential-energy scan followed by an *m*PW1PW91/TZP single-point calculation on the maximum of the scan.

have a substantially higher internal energy when exploring the surface (i.e., intermediates **3** to **6**) than the complexes formed from isopropyl alcohol.[54]

Let us now return to structure **4** and the key role this intermediate is suggested to play in terms of the observed asymmetry in the decay of the *n*-propyl alcohol/Fe^+ complexes (see above). The H/D equilibration requires the partial isomerization of **3** ⇄ **4** as depicted in Scheme 3. For a metal-mediated isomerization of an *n*-propyl to an isopropyl group, one may readily conclude that in the course of the reaction the Fe atom no longer "remembers" the information about its initial interaction with C(1); after all, C(1) and C(3) are expected to become indistinguishable due to the constitutional equivalence of the two methyl groups. On the basis of experiment (see above), this is clearly not the case in the present system. Further, the quantum-chemical calculations also confirm the inherent asymmetry of **4** as postulated above to account for the experimental findings. The nature of this asymmetry becomes apparent in the particularly short distance of iron to one of the β-H atoms (193 pm) in structure **4** (Chart 3). In comparison, the shortest distance between the metal center and any other β-H atom is considerably longer (304 pm). To assess the strength of the agostic stabilization, **TS 4/4′** for the degenerate rearrangement **4** ⇄ **4′** (Scheme 3) is calculated. According to this calculation, it takes about 5 kJ/mol to break the agostic interaction. Thus, it is this very interaction that provides an explanation for the experimentally observed preference for elimination of water with a hydrogen atom which preferentially originates from C(1) and C(2) in the **1**/Fe^+ complexes. Although the internal energy of **4** is by far sufficient to overcome a barrier of 5 kJ/mol, a fraction of the metastable ions formed upon passage of **TS 1/3** may prefer to proceed along the reaction coordinate en route to formation of the products. Obviously, this sort of asymmetry is not observed in the case of **2**/Fe^+, which enters the surface from a precursor with two identical methyl groups. Hence, the chances are equal to form an agostic interaction with either methyl group, and the asymmetry of **4** remains experimentally undetected. While the computational results can thereby qualitatively account for the observed asymmetry in **1**/Fe^+, it remains so far an unresolved puzzle how **1**/Fe^+ can undergo extensive H/D equilibration at the C(1) and C(2) position while the C(3) position contributes to a minor extent. The computed PES can qualitatively account for this observation, while a quantitative analysis of the computed barrier heights of **TS3/5** and **TS4/6** versus **TS4/4′** suggests the opposite. At present, the origin of this discrepancy remains unknown. Perhaps, the DFT algorithms are unable to provide an accurate description of the degenerate rearrangment **4** ⇄ **4′** due to symmetry-breaking problems.

(54) A reviewer has suggested that this aspect may provide an explanation for the experimentally observed memory effect. Thus, the species generated after passage over **TS 1/3** contain more internal energy than those derived from isopropyl alcohol/Fe^+ and have therefore less time to explore the entire potential-energy surface (see also Scheme 3) before dissociation. While a rapid dissociation of the intermediates would indeed account for the inequivalence of the C(1) and C(3) positions, this scenario is not able to explain both experimental observations: the memory effect on one hand and the almost complete equilibration of hydrogen atoms bound to C(1) and C(2) on the other.

Table 6. Relative Rate Constants (k_{exp}/k_{cap})[a] and Product Distributions of the Reaction of FeO^+ with Labeled Propanes[b]

	k_{exp}/k_{cap}	−water	−propyl alcohol	−methyl	−propene
C_3H_8 (**10**)	0.47	44	31	17	8
$CH_3CD_2CH_3$ (**10a**)	0.37	40	25	27	8
$CH_3CH_2CD_3$ (**10b**)	−[c]	39	38	11	12[d]
C_3D_8 (**10c**)	0.46	42	31	22	5

[a] Experimental rate constants (k_{exp}) are given as a percentage of the theoretical collision rate derived from the capture theory (k_{cap}).[63−65] [b] All intensities for different isotopic distributions of the same reaction channel are summed, and the values for the intensities of the product distributions are normalized to $\Sigma = 100$. [c] The synthesized sample contained some residual gases, most probably air and water. Therefore, the measured ratio of $k_{exptl}/k_{cap} = 0.12$ represents a lower boundary. [d] Due to contamination of the sample with traces of water, this reaction channel may be slightly overestimated because of secondary reactions.

Scheme 4

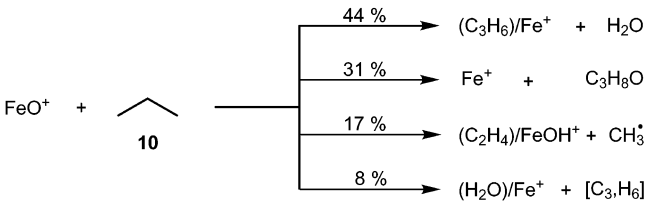

4.4. FeO^+ and Propane. The knowledge acquired in the examination of the propyl alcohol/Fe^+ systems can be used to obtain further insight in the mechanistic details of the reaction of FeO^+ with propane, which has previously been investigated with FTICR-MS.[9,10] These two reactions are closely related, as FeO^+ reacts via insertion into a C−H bond of propane, thus formally leading to the same intermediates as those obtained after insertion of Fe^+ into the C−O bonds of the isomeric propyl alcohols. One of the key questions in this respect concerns the regioselectivity of the initial C−H bond activation by FeO^+, and propane is the simplest substrate with nonactivated C−H bonds in which primary and secondary positions can be distinguished. Understanding of the mechanistic details of chemo- and regioselectivity is of prime importance in the field of selective hydrocarbon functionalization.[55,56]

To this end, FeO^+ was reacted with propane **10** and the deuterated variants **10a**−**c** under the conditions of FTICR-MS (Table 6). In accordance with previous studies,[9,10] the reaction of FeO^+ with propane gives rise to four different ionic products, which are due to losses of water, propene, and a methyl radical as well as oxygen atom transfer to the alkane (Scheme 4). The reactions of the labeled propanes **10a** and **10b** as well as a comparison of **10** with fully deuterated propane (**10c**) do not reveal the operation of particularly strong intermolecular kinetic isotope effects, as $k_{exp}/k_{cap} = 0.47$ (**10**) and $k_{exp}/k_{cap} = 0.46$ (**10c**) agree within the error margins. Because neutral products cannot be detected in these FTICR experiments, the reaction to form Fe^+ via oxygen transfer to the alkane quite unfortunately does not provide any information with respect to the

(55) Olah, G. A.; Molnár, A. *Hydrocarbon Chemistry*; Wiley-Interscience: New York, 1995.

(56) Davies, J. A., Watson, P. L., Liebman, J. F., Greenberg, A., Eds. *Selective Hydrocarbon Activation: Principles and Progress*; VCH: New York, 1990.

Table 7. Isotopic Distribution for the H_2O, HDO, and D_2O Losses in the Reaction of FeO^+ with Isotopically Labeled Propanes Assigned from High-Resolution Spectra[a] and Modeling of the Propane/FeO^+ System

	10a		10b	
	exptl	model[b]	exptl	model
$-H_2O$	24.0 ± 0.4	23.9	53.5 ± 0.2	53.6
−HDO	74.9 ± 0.4	75.1	43.0 ± 0.2	42.0
$-D_2O$	1.0 ± 0.2	1.0	4.5 ± 0.2	4.4

[a] Spectra are normalized to $\sum = 100$. The error stated represents the standard deviation of the spectra measured at different reaction times. [b] Parameters: $f_{prim} = 0.77 \pm 0.01$, $f_s = 0.56 \pm 0.03$, $KIE_{ins} = 1.31 \pm 0.14$, $KIE_s = 1.11 \pm 0.06$, $KIE_x = 1.28 \pm 0.24$, and $c_{as} = 0.4 \pm 0.1$.

regioselectivity of C−H bond activation. The methyl-radical elimination in the propane/FeO^+ system reveals—though indirectly—an unusually high selectivity. As suggested earlier,[10] FeO^+-mediated carbon−carbon bond scission is preceded by activation of a C−H bond located in a position β to the C−C bond to be cleaved. Thus, for the substrate $CH_3CH_2CD_3$ (**10b**), the loss of $CH_3^\bullet$ is initiated by the activation of a primary C−D bond, while elimination of $CD_3^\bullet$ requires the activation of a primary C−H bond. The $CH_3^\bullet/CD_3^\bullet$ ratio measured for **10b**/FeO^+ amounts to 35.4 ± 0.4/64.6 ± 0.4; losses of $CH_2D^\bullet$ and $CHD_2^\bullet$ were not observed. In analogy to the *n*-propyl alcohol/Fe^+ system, loss of a methyl radical is not affected by any H/D equilibration, and consequently this reaction commences only with activation of a primary carbon−hydrogen bond. Further, the $CH_3^\bullet/CD_3^\bullet$ ratio provides a first approximation to the kinetic isotope effect operative in the C−H versus C−D bond activation. Neglecting that the product distribution may be influenced by secondary isotope effects, the $CH_3^\bullet/CD_3^\bullet$ ratio translates to a KIE_{ins} value of 1.82 ± 0.03 for the initial insertion of FeO^+ into a primary C−H bond of propane.[57] Loss of propene as a minor reaction channel (8%) by and large reflects the isotope distribution pattern of the major channel, leading to the evaporation of water.[58] The complementary behavior of the water and propene eliminations is consistent with the assignment that both $(C_3H_6)Fe^+$ and $(H_2O)Fe^+$ result from the bis-ligated complex **7**. Therefore, the subsequent quantitative analysis is restricted to the ratios of $H_2O/HDO/D_2O$ losses, as these are the most accurate data available (Table 7).

A first and obvious conclusion from the experiments is that extensive H/D equilibration occurs in the course of propane activation, because the two deuterated propanes **10a** and **10b** lose H_2O, HDO, and D_2O in competition. While this finding is in pleasing analogy with the chemistry observed for the isomeric propyl alcohol/Fe^+ systems, the H/D equilibration masks information about the regioselectivity of the initial C−H bond activation in propane by FeO^+.

For a quantitative analysis of the product distributions generated from propane/FeO^+ analogous to the propyl alcohol/Fe^+ systems, additional parameters are required to express the regioselectivity of the initial C−H bond activations as well as the associated KIEs. Accordingly, for a reliable modeling an even larger set of selectively deuterated propanes was required. The higher symmetry of propane compared to the corresponding propyl alcohols, however, imposes a principal restriction to such an approach in that not as many different deuteration patterns as required are available. For example, C−H(D) bond activation of [1,1,1-D_3]-propane (**10b**) by FeO^+ can conceptually give rise to a mixture of three propyl alcohol/Fe^+ isomers as well as the associated insertion intermediates. Likewise, two different isomers can arise from [2,2-D_2]-propane/FeO^+ (Scheme 5). As the number of parameters clearly exceeds those directly available from the experimental data, some conceptual information from the propyl alcohol/Fe^+ needs to be adopted in an attempt to kinetically model the propane/FeO^+ system. Further, two additional parameters are required for propane/FeO^+. One represents the fraction of the reaction that takes place after activation of a primary C−H bond (f_{prim}), which also defines the fraction involving the activation of a secondary C−H bond ($f_{sec} = 1 - f_{prim}$). The second parameter is KIE_{ins}, associated with the insertion of FeO^+ into a C−H(D) bond; here, for the sake of simplicity the same KIE_{ins} is assumed to be operative for the insertions in either primary or secondary C−H bonds. This is, perhaps, an oversimplification.

Scheme 5

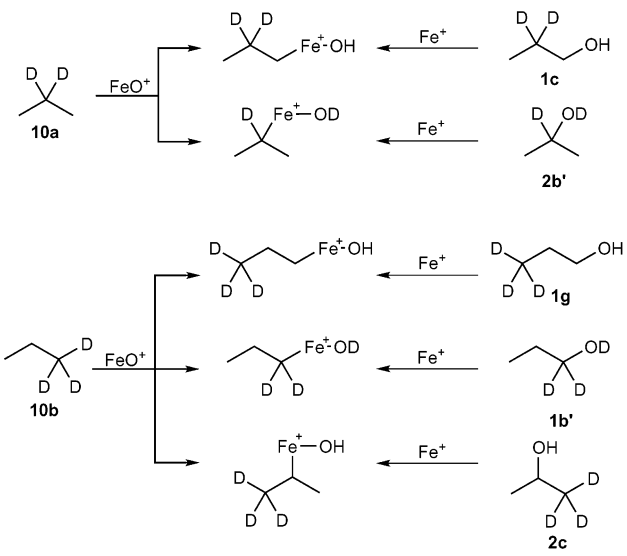

In a first approach, it is probed whether the dehydrations of **10**/FeO^+, **1**/Fe^+, and **2**/Fe^+ are related closely enough to justify that the parameters derived for the propyl alcohol/Fe^+ systems can be adopted for **10**/FeO^+. To this end, let us consider the insertion products of the two investigated isotopically labeled propanes $CH_3CD_2CH_3$ (**10a**) and $CH_3CH_2CD_3$ (**10b**), which correspond to the insertion products of Fe^+ and the appropriate propyl alcohols (Scheme 5). Three of these labeled propyl alcohols (**1c**,**g** and **2c**) have been measured, and their H_2O/HDO ratios are known (Table 1). The two missing propyl alcohols, **1b′** and **2b′**, differ from **1b** and **2b** only with regard to the presence of a deuterium atom in the hydroxyl groups. Because the hydroxyl group is clearly not involved in any H/D exchange (see above), the expected HDO/D_2O ratios of $CH_3CH_2CD_2OD/Fe^+$ and

(57) For related examples to derive KIEs of multistep gas-phase ionic processes, see: Schwarz, H. *Top. Curr. Chem.* **1981**, *97*, 1 and references therein.

(58) The analysis of the isotope distribution of this particular channel is hampered by rapid exchanges of the products $(HDO)/Fe^+$ and $(D_2O)/Fe^+$ with background water.

$CH_3CD(OD)CH_3/Fe^+$ can be derived directly from **1b**/Fe^+ and **2b**/Fe^+. If the parameters for propane/FeO^+ can indeed be adopted from the propyl alcohol/Fe^+ systems, the H_2O/HDO/D_2O ratios for the labeled propanes should be reproducible by linear combinations of the corresponding H_2O/HDO and HDO/D_2O ratios derived from the propyl alcohol/Fe^+ complexes. However, irrespective of the choice of f_{prim} and KIE_{ins}, no satisfactory modeling of the experimentally measured ratios is obtained. In fact, qualitative considerations imply that the dehydration of **10**/FeO^+ is more selective than the reactions of Fe^+ with *n*-propyl and isopropyl alcohol, probably due to shorter lifetimes of the resulting insertion intermediates emerging from the larger overall energy content of FeO^+ and propane ($\sum\Delta_f H = 173$ kJ/mol) vs Fe^+ + propyl alcohol ($\sum\Delta_f H = 119$ kJ/mol and $\sum\Delta_f H = 101$ kJ/mol for **1** and **2**, respectively).[50]

As the parameters of the propyl alcohol/Fe^+ systems cannot be adopted for the reaction of FeO^+ with propane, we attempted to derive an alternative set of equations to model the experimental H_2O/HDO and H_2O/D_2O ratios for **10a**/FeO^+ and **10b**/FeO^+. While the model is still based on the findings for the reactions of Fe^+ with *n*-propyl and isopropyl alcohol, we deliberately avoided adopting the values of the corresponding parameters (f_s, KIE_s, KIE_x, and c_{as}). For **10a**/Fe^+, this model results in eqs 6 and 7 for the H_2O/HDO and H_2O/D_2O ratios, respectively. Likewise, the H_2O/HDO and H_2O/D_2O ratios of **10b**/FeO^+ are expressed by eqs 8 and 9, respectively. Unfortunately, the set of equations is underdetermined and cannot be solved by simply fitting all parameters to the experimental data. However, the set of equations can be augmented by one further equation, because the intermolecular isotope effect is known and allows the measurements of **10a**,**b** (eq 10) to be interrelated. Theoretically, the conjunction between **10a** and **10b** can be expressed by relating the H_2O, the HDO, or the D_2O losses, respectively. Unfortunately, that does not leave us with three more equations but only one, as the information that can be gained from the other two equations is redundant. In this case the D_2O ratios are chosen because most parameters cancel out and eq 10 reveals directly that, irrespective of the other parameters, f_{prim} can only vary between $f_{prim} = 0.72$ ($c_{as} = 1$) and $f_{prim} = 0.82$ ($c_{as} = 0$).

$$\frac{H_2O}{HDO} = \frac{f_{prim}\left[(1-f_s)\frac{2+3c_{as}}{4+3c_{as}}\right]}{f_{prim}\left[\frac{f_s}{KIE_s}+\frac{(1-f_s)}{KIE_x}\times\frac{2}{4+3c_{as}}\right]+\frac{1-f_{prim}}{KIE_{ins}}\left[f_s+(1-f_s)\frac{6}{7}\right]} \quad (6)$$

$$\frac{H_2O}{D_2O} = \frac{f_{prim}\left[(1-f_s)\frac{2+3c_{as}}{4+3c_{as}}\right]}{\frac{(1-f_{prim})}{KIE_{ins}}\left[\frac{1-f_s}{KIE_x}\times\frac{1}{7}\right]} \quad (7)$$

$$\frac{H_2O}{HDO} = \frac{A}{B} \quad (8)$$

$$A = \frac{1}{2}f_{prim}\left[f_s+(1-f_s)\frac{4}{4+3c_{as}}\right]+(1-f_{prim})\left[\frac{1}{2}f_s+(1-f_s)\frac{4}{7}\right]$$

$$B = \frac{f_{prim}}{2KIE_{ins}}\left[f_s+(1-f_s)\frac{2+3c_{as}}{4+3c_{as}}\right]+\frac{f_{prim}}{2}\times\frac{1-f_s}{KIE_x}\times\frac{3c_{as}}{4+3c_{as}}+(1-f_{prim})\left[\frac{f_s}{2KIE_s}+\frac{1-f_s}{KIE_x}\times\frac{3}{7}\right]$$

$$\frac{H_2O}{D_2O} = \frac{\frac{1}{2}f_{prim}\left[f_s+(1-f_s)\frac{4}{4+3c_{as}}\right]+(1-f_{prim})\left[\frac{1}{2}f_s+(1-f_s)\frac{4}{7}\right]}{\frac{f_{prim}}{2KIE_{ins}}\frac{1-f_s}{KIE_x}\frac{2}{4+3c_{as}}} \quad (9)$$

$$\frac{D_2O(\mathbf{10a})}{D_2O(\mathbf{10b})} = \frac{1-f_{prim}}{f_{prim}}\times\frac{4+3c_{as}}{7} \quad (10)$$

Despite eq 10, the set of equations is still underdetermined by one equation. To obtain a first-order solution, one parameter (c_{as}) is kept constant and varied manually between 0 and 1. Since we are only interested in physically meaningful solutions, the possible range for c_{as} can be specified further. As there is no obvious reason the KIE for the 1,2-elimination should be inverse, we will only consider values for c_{as} which yield normal KIEs. The results of this procedure are shown in Table 7. The degree of selective 1,2-elimination amounts to (56 ± 3)% with a KIE_s value for this reaction of 1.11 ± 0.06. With respect to the regioselectivity of the initial C−H bond activation—one of the key questions in this context—the results indicate that (77 ± 1)% of the FeO^+ insert into a primary C−H bond of propane and (23 ± 1)% activate a secondary C−H bond. Considering the fact that there are six primary but only two secondary C−H bonds in the propane molecule and correcting for this statistical weight, it follows that there is practically no significant ($(52.7 \pm 1.5\%)_{prim}$:$(47.3 \pm 1.5\%)_{sec}$) selectivity in the initial C−H bond activation of propane by bare FeO^+. Interestingly, however, if any selectivity can be derived from these values, it is in favor of the activation of primary C−H bonds, which can perhaps be attributed to the better accessibility of the primary C−H bonds in propane by the FeO^+ species.

5. Conclusions

Quantitative kinetic modeling of the unimolecular reactions of metastable *n*-propyl and isopropyl alcohol/Fe^+ complexes provides detailed insight into the reversible bond activations operative in the course of metal-mediated H/D equilibration. A key result of the modeling is that the insertion intermediates involved are characterized by agostic interactions which not only energetically stabilize the intermediates but also impose some asymmetry to formally constitutionally identical methyl groups of an isopropyl residue generated from an *n*-propyl backbone. As a result, despite the fact that extensive H/D equilibration precedes the dissociation of *n*-propyl alcohol/Fe^+, the metastable ion mass spectra exhibit a memory effect with regard to the initial

structure. Density functional calculations lend qualitative support to this interpretation, in that the reaction pathways for *n*-propyl alcohol/Fe^+ and isopropyl alcohol/Fe^+ only merge completely in the quasi-irreversible formation of the bis-ligated product complex **7**. The quantitative agreement is less pleasing, however, because the computed energetics suggest a rapid interconversion of the various agostic structures, whereas the experimental data imply a more pronounced kinetic restriction. Notwithstanding, successful kinetic modeling of the experimental data demonstrates that a quantitative analysis of seemingly random isotope distributions can provide valuable information with regard to subtle mechanistic details.

For the related reaction of FeO^+ with propane, the analysis is less stringent because several approximations and assumptions are to be made. Nevertheless, the results indicate that there is no intrinsic selectivity of bare FeO^+ with respect to the activation of primary versus secondary C−H bonds in propane. This result corroborates the previous suspicion that the bare FeO^+ ion, which is even capable of activating methane,[10] is too reactive to allow for selective bond activations of more complex alkanes. A somewhat different situation arises, however, in the case of functionalized alkanes, where the functional groups may serve as a docking site for the reactive cationic species, thereby giving rise to certain preferred trajectories for the subsequent intramolecular bond-activation steps.[59,60]

The results presented in this work may also help in uncovering some mechanistic aspects of transition-metal-catalyzed polymerizations and hydrations of alkenes, in which agostic interactions control the product distributions to some extent.[61] Similarly, the concept of β-agostic interaction may explain some of the puzzling results of intramolecularly controlled catalytic hydrogenations[62] where structural memory effects have been invoked. Agostic interactions, which have not been considered explicitly, may well serve to provide an alternative rationale for the experimental observations.

Acknowledgment. This work was supported by the Deutsche Forschungsgemeinschaft and the Fonds der Chemischen Industrie. The Konrad-Zuse-Zentrum, Berlin, is acknowledged for generous allocation of computer time, and helpful comments by the reviewers are appreciated.

OM020893Z

(59) Schwarz, H. *Acc. Chem. Res.* **1989**, *22*, 282.
(60) Schröder, D.; Heinemann, C.; Koch, W.; Schwarz, H. *Pure Appl. Chem.* **1997**, *69*, 273.
(61) Tempel, D. J.; Johnson, L. K.; Huff, R. L.; White, P. S.; Brookhart, M. *J. Am. Chem. Soc.* **2000**, *122*, 6686.
(62) Brown, J. M. *Angew. Chem., Int. Ed. Engl.* **1987**, *26*, 190.
(63) Su, T.; Chesnavich, W. J. *J. Chem. Phys.* **1982**, *76*, 5183.
(64) Su, T. *J. Chem. Phys.* **1988**, *88*, 4102.
(65) Su, T. *J. Chem. Phys.* **1988**, *89*, 5355.